

PHASE RECOVERY FOR TIME OF ARRIVAL ESTIMATION IN THE PRESENCE OF INTERFERENCE

Kevin Nguyen^{*} David Humphrey[†] Mark Hedley[†] Philip H.W Leong^{*}

^{*}School of EIE, The University of Sydney, Sydney Australia

[†]CSIRO Digital Productivity Flagship, Sydney Australia

^{*}kngu8473@uni.usyd.edu.au, philip.leong@sydney.edu.au

[†]dave.humphrey@csiro.au, mark.hedley@csiro.au

ABSTRACT

Time of arrival is a commonly used mechanism for geolocation. In many environments, multipath propagation of RF signals limits accuracy. Wide bandwidths reduce the impact of multipath propagation, but frequently results in interference from other devices. When the bandwidth is assembled from several measured sub-bands, there is an additional difficulty of a random phase offset between bands. In this paper, we introduce a compressive sensing scheme which recovers both corrupted samples and phase offsets between sub-bands. For interferers with bandwidths up to 12 MHz, we further show that the proposed scheme leads to improved localisation accuracy compared to previously published techniques.

Index Terms— Compressed sensing, Time of Arrival

1. INTRODUCTION

The performance of time of arrival (TOA) based positioning is degraded by multipath propagation [1, 2]. To address this issue, large bandwidths are often used to make it easier to resolve multipath components. A number of systems have been proposed using wideband (>100 MHz) and ultra wideband (>500 MHz) radios. However, many commercially available radios cannot access all available frequency bands using a single radio transmission. Even if it is possible, other users of the same spectrum may interfere over some sub-bands. Since the accuracy of TOA based localisation is inversely proportional to the total bandwidth [3], the ability to use non-contiguous blocks of spectrum can result in substantial improvement in the positioning accuracy.

An example of a TOA based implementation is the Wireless Ad-hoc System for Positioning (WASP) [3], which is a wideband device that makes use of the Industrial, Scientific and Medical (ISM) class license band. The ISM band offers bandwidths of 83 MHz at 2.4 GHz and 125 MHz at 5.8 GHz which can be used for TOA estimation. However, other wireless devices such as Bluetooth, cordless phones and WLANs also use this spectrum, introducing interference which may have bandwidths ranging from a few MHz to 20 MHz or more. Ultra wideband systems (e.g. Zebra Dart [4], Ubisense [5]) have lower power and wider bandwidth making them very susceptible to interference.

Many standards such as WiFi and 3G or 4G mobile systems allow the use of multiple different frequency bands, which may not be contiguous. TOA estimation can be substantially improved for such devices if they can be made to use all the available spectrum. The market penetration of TOA based positioning could be improved

dramatically if accurate TOA could be made to work on such widely available commercial radios.

One key issue not addressed in other work [11] is the recovery of the phase offset between channel estimates in different frequency bands. In order to cover a wide band, most commercial radios need to be retuned to multiple different frequency bands. However, the retuning process involves resetting a phase locked loop which induces a random phase shift between channel estimates made in the two different frequency bands. Consider the use of a standard 802.11 radio. This will provide up to 80 MHz of bandwidth (for current 11ac devices), which can be tuned to one of 5 different centre frequencies in the 5.2 to 5.8GHz range. The radio will estimate the channel across 108 OFDM subcarriers with each band, so even if two adjacent frequency bands are used, there will be a gap of 12.5 MHz between the high frequency subcarrier estimated in the lower band and the lowest frequency subcarrier estimated in the higher band. Furthermore, 802.11 networks often have to coexist with other devices (or other 802.11 networks) which may mean that portions of the band are inaccessible (for example, an 802.11g network may occupy about 16 MHz of spectrum in the middle of the band).

There is wide body of work on the problem of accurate TOA estimation. The authors of [6] proposed an energy detector based TOA estimation scheme, where a comparison between the output of the energy detector and a threshold is used to determine the first arriving path. Other schemes such as the Maximum likelihood criterion with iterative interference cancellation [7] and compressive sensing methods have been used for channel estimation [8, 9, 10]. Unfortunately, none of these techniques attempt to solve the problem of phase recovery between different frequency bands.

In this paper, we build on the research of [11] to include the ability to find the optimal phase shift for segmented frequency bands. Using compressive sensing methods, we can estimate the corrupted channel frequency samples [12].

The paper is organised as follows. Section II reviews the previous research. In section III, we view the proposed algorithm for interference mitigation and how phase shift estimation is fitted into the existing framework. In section IV, we present our results for the proposed algorithm.

2. BACKGROUND

In [11], reconstruction of corrupted frequency sub-bands via L_1 minimization was proposed. In the presence of narrowband interference, the channel frequency response can be thought of as a non-uniform sampling of the true frequency response. Using compressive sensing, the missing samples can be estimated from the incomplete fre-

quency response [13]. The technique is summarised in this section.

The multipath impulse channel can be modelled as:

$$h(t) = \sum_{t=0}^{p-1} a_i \delta(t - \tau_i) \quad (1)$$

where a_i is the amplitude of the signal, p is the number of paths, τ_i is the time delay associated with each signal path and δ is the delta function. Equation (1) then can be re-written in the Fourier domain as:

$$H(f) = \sum_{t=0}^{p-1} a_i e^{-j2\pi\tau_i f} \quad (2)$$

Given $H(f)$, the channel impulse can be approximated by taking the inverse discrete Fourier transform (iDFT) of the signal, that is:

$$h(t) = F * H(f) \quad (3)$$

where F is the iDFT matrix. We can decompose (3) into smaller sub matrices, by considering the channel impulse response $h(f)$ as containing samples that are close to zero h^z and samples that are non zero h^{nz} . We can also divide the frequency response $H(f)$ into sections that have been measured H^m and sections that is corrupted due to interference H^i . If we also permute the iDFT matrix accordingly, then (3) can be written as:

$$\begin{bmatrix} h^z \\ h^{nz} \end{bmatrix} = \begin{bmatrix} F^{z,m} & F^{z,i} \\ F^{nz,m} & F^{nz,i} \end{bmatrix} \begin{bmatrix} H^m \\ H^i \end{bmatrix} \quad (4)$$

Because h^z is close to zero, the unknown frequency samples H^i then can be recovered by finding the solution to the minimization problem

$$\min_{H^i} \|F^{z,m} H^m + F^{z,i} H^i\| \quad (5)$$

Equation (5) is minimized using the L_1 norm which is preferred because it is more robust against outliers. It can be recast as a linear programming problem and solved using an interior point method. For this work, L_1 -magic was used [16].

Selection of which samples, $h(t)$, go into h^z and h^{nz} is determined iteratively by first selecting an interval $[\tau_1, \tau_2]$ that is wide enough to contain the impulse response. All samples between $[\tau_1, \tau_2]$ are placed into h^{nz} and all samples outside the interval are placed into h^z . Equation (5) can then be solved, after which the amplitude of the samples outside the intervals $[\tau_1, \tau_2]$ are compared to a threshold. If the amplitudes are less than the threshold, the intervals are reduced and the process is repeated. If samples before τ_1 are above the threshold then τ_1 is reduced, similarly if any samples after τ_2 are above the threshold then τ_2 is increased. The algorithm concludes when we can no longer reduce the interval $[\tau_1, \tau_2]$ without exceeding the threshold. At this point, we have recovered our H^i samples for a complete channel frequency response $H(f)$.

3. INCLUSION OF PHASE OFFSET

In order to consolidate the segmented and phase incoherent bands, not only do we have to fill the gap, we also need to introduce an appropriate phase shift. In this section we present a technique for interference mitigation with phase offset.

3.1. The L_1 Minimization Problem

Our measured frequency response samples H^m are divided into separate sub-bands according to the location of the gap. Assuming a single gap, H^m can be divided into H^{m_1} and H^{m_2} . We can introduce a phase shift θ so the problem can be rewritten as

$$\min_{H^i, \theta} \left\| F^{z,m_1} H^{m_1} + \begin{bmatrix} F^{z,i} & F^{z,m_2} H^{m_2} \end{bmatrix} \begin{bmatrix} H^i \\ e^{i\theta} \end{bmatrix} \right\| \quad (6)$$

Once again, the iDFT matrices F are split accordingly. The phase of H^{m_1} is taken to be the reference to which H^{m_2} must align. Equation (6) can now be generalized for the case where there is more than one gap in the spectrum, each separate sub-band having its own phase shift θ_i :

$$\min_{H^i, \theta} \left\| F^{z,m_1} H^{m_1} + \gamma \begin{bmatrix} H^i \\ e^{i\theta_1} \\ e^{i\theta_2} \\ \vdots \\ e^{i\theta_{s-1}} \end{bmatrix} \right\| \quad (7)$$

where γ is $\begin{bmatrix} F^{z,i} & F^{z,m_2} H^{m_2} & \dots & F^{z,m_s} H^{m_s} \end{bmatrix}$ and s is the number of frequency sub-bands.

3.2. Linearizing the Problem

In (6), the phase shift variable θ introduces a non-linear component ($e^{i\theta}$). We can linearize this by finding the tangent vector to a point on the unit circle in the complex plane corresponding to $e^{i\theta}$. We define the tangent vector as

$$\zeta = z_0 + \alpha r \quad (8)$$

where z_0 is the position vector, α is the direction vector, and r is a real number. We can now replace $e^{i\theta}$ with ζ in (6) to get

$$\min_{H^i, r} \left\| F^{z,m_1} H^{m_1} + F^{z,i} H^i + \zeta F^{z,m_2} H^{m_2} \right\| \quad (9)$$

$$= \min_{H^i, r} \left\| F^{z,m_1} H^{m_1} + F^{z,i} H^i \quad (z_0 + \alpha r) F^{z,m_2} H^{m_2} \right\| \quad (10)$$

$$= \min_{H^i, r} \left\| \eta + \begin{bmatrix} F^{z,i} & \alpha F^{z,m_2} H^{m_2} \end{bmatrix} \begin{bmatrix} H^i \\ r \end{bmatrix} \right\| \quad (11)$$

where $\eta = F^{z,m_1} H^{m_1} + z_0 F^{z,m_2} H^{m_2}$

Normally, introducing a phase shift would not affect the amplitude of the frequency samples. Because the problem is linearized, the magnitude of ζ is not equal to 1. This changes the amplitude of the frequency samples slightly.

3.3. Algorithm

The overall approach is described in Algorithm 1. H is the current frequency response with the gap filled by H^i . h and h_p are the impulse corresponding to H and H_{best} , respectively. The inner loop begins by selecting ζ to be an initial value of 1. After appropriately selecting an interval $[\tau_1, \tau_2]$, we solve (11) to obtain our phase offset and unknown frequency samples (r and H^i) via L_1 norm minimization; a primal-dual algorithm for linear programming implemented in L_1 -magic was used. For a pure phase shift, it must follow that $\|\zeta\| = 1$. However we allow some slack in this condition i.e., $1 \leq \|\zeta\| < 1 + \beta$ where β is chosen to be 0.01 or smaller. We check

the samples outside $[\tau_1, \tau_2]$ and adjust the interval accordingly. After that we also check to see if $\|\zeta\| < 1 + \beta$ is satisfied. If it isn't then we find the new tangent vector at point $e^{i \arg(\zeta)}$ and reiterate. The inner loop terminates when $[\tau_1, \tau_2]$ can no longer be reduced and $\|\zeta\| < 1 + \beta$ is satisfied.

The outer loop allows the algorithm to start with 5 different θ values, spaced evenly around the unit circle. At every iteration, τ_1 is compared to τ_{1p} (the previous interval's start point), which is initially set to 0. If $\tau_1 > \tau_{1p}$, then the current solution to equation (11) is kept, otherwise it is discarded. In the case that $\tau_1 = \tau_{1p}$, the solution which yields the smallest L_1 norm is kept. The outer loop is needed as sometimes the algorithm finds a local minima in the optimization problem. Several starting points are used to increase its performance.

Algorithm 1 Phase recovery algorithm

```

Initialize  $\tau_1, \tau_2$  to appropriate values,  $\tau_{1p} = 0$ 
for k := 0:4 do
   $\zeta \leftarrow$  new  $\zeta$  corresponding to the point at  $e^{i\pi k \times 0.4}$ 
  while  $\|\zeta\| \geq 1 + \beta$  and (stop left and stop right)  $\neq$  true do
    solve equation (11)
    if  $h^z$  samples before  $\tau_1 <$  threshold and stop left = false
      then
        increase  $\tau_1$ 
    else
      decrease  $\tau_1$ 
      stop left  $\leftarrow$  true
    end if
    if  $h^z$  samples after  $\tau_2 <$  threshold and stop right = false
      then
        decrease  $\tau_2$ 
    else
      increase  $\tau_2$ 
      stop right  $\leftarrow$  true
    end if
    if  $\|\zeta\| \geq 1 + \beta$  then
       $\zeta \leftarrow$  new  $\zeta$  corresponding to the point at  $e^{i \arg(\zeta)}$ 
    end if
  end while
  if  $\tau_1 > \tau_{1p}$  or ( $\tau_1 = \tau_{1p}$  and  $\|h\|_1 < \|h_p\|_1$ ) then
     $H_{best} \leftarrow H$ 
     $\tau_{1p} \leftarrow \tau_1$ 
  end if
end for
return  $(\tau_1, \tau_2, \zeta, H_{best})$ 

```

4. RESULTS

The algorithm was tested using channel frequency responses recorded in an indoor office environment using the WASP system. Two different scenarios are considered, a non line of sight (NLOS) situation (with two walls between the transmitter and receiver) and a line of sight (LOS) situation. To simulate the effects of a gap in the spectrum, an appropriate number of frequency domain samples were omitted.

We are interested in the reconstruction of the leading edge as this affects TOA estimation. In figure 1, the root mean square error (RMSE) of the leading edge with gap sizes ranging between 0.3906MHz to 16 MHz was measured. The interferer was placed at 5800 MHz. Random phase offsets were introduced to the higher

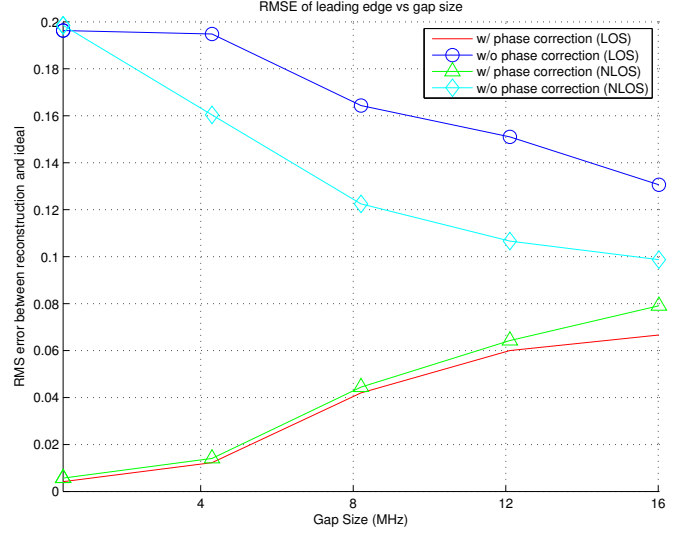


Fig. 1. The first significant peak of the ideal impulse response is scaled to one, the recovered impulse responses were scaled accordingly.

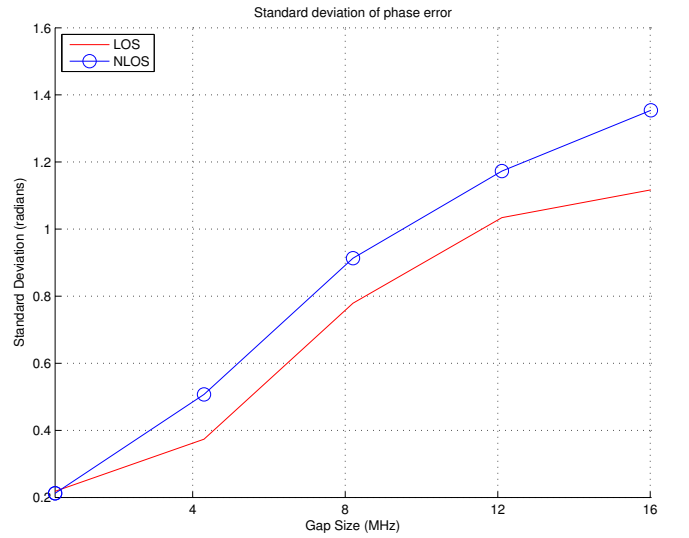


Fig. 2. Standard deviation of phase estimation error for both line of sight and non line of sight conditions.

segmented band of the frequency spectrum. Without phase correction, the reconstruction of the leading edge exhibits large errors. The RMSE without phase correction reduces as the interferer bandwidth increases. This is because with a small gap size, a random phase offset between the two frequency bands will result in large step change in the phase which leads to a noisy impulse response. With larger gap sizes the impact of a random phase offset is reduced as the algorithm is able to fill in a smooth change between the bands. With phase correction, there is a considerable decrease in RMSE which will directly benefit TOA estimations. As the gap size increases, the algorithm struggles to find the true phase shift; hence the increase in RMSE.

Both the recovery of the missing spectrum and the recovery of

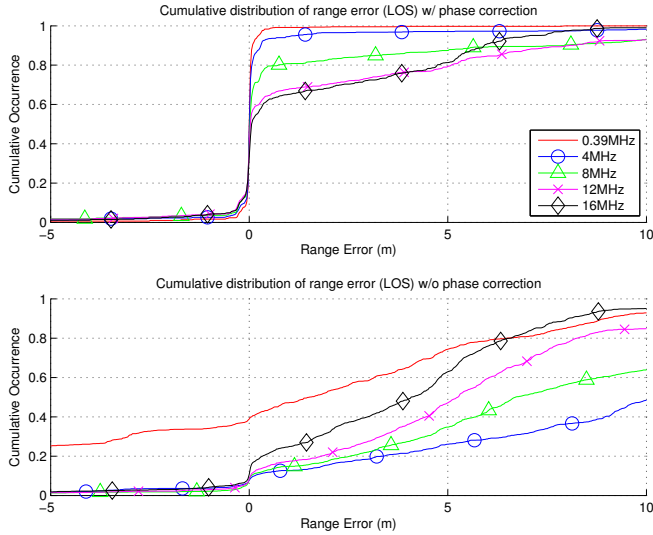


Fig. 3. Cumulative distribution error for line of sight conditions.

the phase offset between the bands becomes more difficult as the size of the gap increases. Figure 2 shows a rise in standard deviation of phase error as the gap size increases. Note that an average phase error of $\pi/2$ is expected if the recovered phase is random (i.e., unrelated to the true phase).

We also calculated the difference between the TOA estimates using the uncorrupted and recovered channel frequency responses [14, 15]. Cumulative error distributions are shown in figure 3 and 4. Note that the range errors shown are additional to the errors in the TOA estimate using the uncorrupted data. The TOA algorithm applied to the uncorrupted data results in range errors of about 40 cm for the LOS case and 80 cm for the NLOS case. As expected, the error gets larger with increasing gap sizes. Even though the phase estimation degrades with larger gap sizes, the algorithm still performs better than without phase correction. This is mainly due to better reconstruction of the leading edge, which can be seen in figure 5. In both figures 3 and 4, the benefits of phase correction is clear for gap sizes of 12 MHz and smaller.

5. CONCLUSION

We have presented a new algorithm that allows increased accuracy for TOA-based ranging, and hence localization, by reconstructing the gap and correcting the phase offset when disjointed and phase incoherent bands are being used. Our results demonstrate a reduction in ranging errors exceeding 1 m from 90% to less than 20% for an 8 MHz interferer.

Acknowledgment

The authors acknowledge support from Marc Durrenburger, Alija Kajan and Phil Ho at the CSIRO for assistance in capturing the data used in the experiments in this paper.

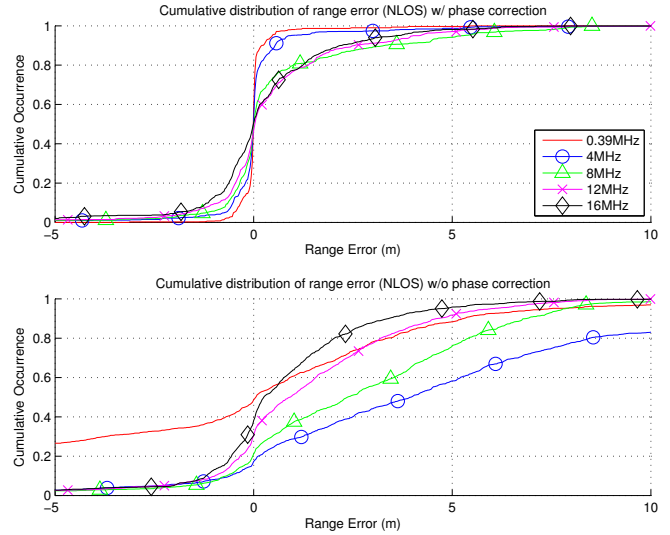


Fig. 4. Cumulative distribution error for non line of sight conditions.

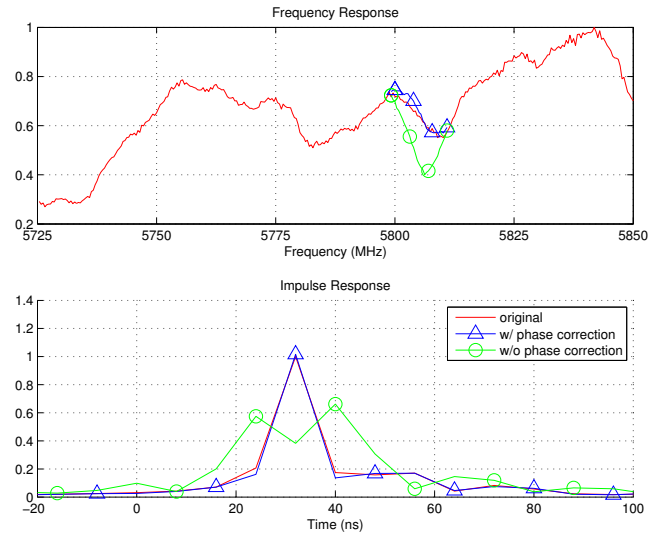


Fig. 5. Comparison of the frequency responses and their corresponding impulse response. This was with a 12 MHz gap at 5800 MHz to 5812 MHz and with a random phase offset. Data used was collected in line of sight conditions.

6. REFERENCES

- [1] S. Gezici, Z. Tian, G. B. Giannakis, H. Kobayashi, A. F. Molisch, H. V. Poor, and Z. Sahinoglu, "Localization via Ultra-Wideband Radios", *IEEE Signal Processing Magazine*, vol. 11, July 2005, pp. 70-83.
- [2] N. Patwari, J. N. Ash, S. Kyperountas, A. Hero, R. L. Moses, N. S. Correal, "Locating the Nodes", *IEEE Signal Processing Magazine*, vol 22, July 2005, pp. 54-69
- [3] M. Hedley, P. Ho, Humphrey, A. Kajan, A. Grancea and K. Pathikulangara, "A Platform for Radio Location Research in Ad Hoc and Sensor Networks", *Proc. IEEE International Sympo-*

sium on Communications and Information Technologies, Sydney, Oct. 2007

- [4] Zebra DART UWB-based Real-Time Location Systems. <http://www.zebra.com/>
- [5] Ubisense Company <http://www.ubisense.net>
- [6] D. Dardari, A. Giorgetti and M. Z. Win, "Time-of-Arrival Estimation of UWB Signals in the Presence of Narrowband and Wideband Interference", *IEEE International Conference on Ultra-Wideband*, Singapore, Sept. 2007, pp. 71-76
- [7] A. G. Amigo, A. Mallat and L. Vandendorpe, "Multiuser and Multipath Interference Mitigation in UWB TOA Estimation", *IEEE International Conference on Ultra-Wideband*, Bologna, Sept. 2011, pp.465-469
- [8] T. N. Le, J. Kim and Y. Shin, "An Improved ToA Estimation in Compressed Sensing-based UWB Systems", *IEEE International Conference on Communications Systems*, Singapore, Nov. 2010, pp.249 - 253
- [9] E. Lagunas and M.Najar, "Sparse Channel Estimation based on Compressed Sensing for Ultra WideBand Systems", *IEEE International Conference on Ultra-Wideband*, Bologna, Sept. 2011, pp. 365-369
- [10] S. Wu, Q. Zhang, H. Yao and Q. Zhang, "High-resolution TOA estimation for IR-UWB ranging based on low-rate compressed sampling", *International ICST Conference on Communications and Networking in China*, Harbin, Aug. 2011, pp.478-483
- [11] D. Humphrey, M. Hedley, "Interference Mitigation for Time of Arrival Estimation", *IEEE Wireless Communications and Networking Conference*, Sydney, April. 2010, pp. 1-6
- [12] R. Baraniuk, "Compressive Sensing", *IEEE Signal Processing Magazine*, 24(4), pp.118-121, July 2007
- [13] E. Candes, J. Romberg, "Robust uncertainty principles: Exact recovery from highly incomplete Fourier information", *IEEE Transactions on information theory*, 52(2), pp.489-509, February. 2006
- [14] D. Humphrey and M. Hedley, "Super-resolution time of arrival for indoor localization", *IEEE International Conference on Communications ICC*, May 2008, pp. 3286-3290
- [15] D. Humphrey and M. Hedley, "Prior Models for Indoor Super-Resolution Time of Arrival Estimation", *IEEE Vehicular technology conference*, April 2009
- [16] J. Romberg, " L_1 -Magic", <http://users.ece.gatech.edu/justin/l1magic/>